Eng. & Tech. Journal, Vol.28, No. 1, 2010

Synthesis And Biological Activity Studies of Some Novel Metal Complexes Derivate From 2-(2-Imino-1-Methylimidazolidin-4-Ylidene) Hydrazinecarbothioamide

Dr. Ahmed Abdulamier Hussain Alamiery* & Dr. Ali A. Juwaied*

Received on:1/3/2009
Accepted on:3/9/2009

Abstract

2-(2-imino-1-methylimidazolidin-4-ylidene)hydrazinecarbothioamide react with chlorides of Cr(III), Co(II), Ni(II) and Cu(II) to yield metal ion complexes of definite composition. These compounds were characterized by elemental analyses, magnetic susceptibility measurements, UV-visible, ^{1}H-NMR and FT-IR spectral investigations. The ligand was studied by using of theoretical method (Simi empirical AMI module in the CS ChemOffice molecular modeling package) by calculation of heat of formation, bond length, bond angle and dihedral angle. The stability for the prepared complexes was studied theoretically by the Density Function Theory (DFT). The free ligand and their metal complexes have been tested *in vitro* against a number of micro-organisms (*Staphylococcus aureus, E. coli, Proteus vulgaris, Pseudomonas, and Klebsiella pneumoniae*), in order to assess their antimicrobial activities. The ligand and its complexes showed considerable activity against all bacteria.

Keywords: bidentate ligand, carbothioamide, metal complexes, spectral investigations

تحضير ودراسة معقدات بعض العناصر الانتقالية المشتقة من 2-(2-ايمينو-1-مثيل ايميدازولدين-4-يل ادين) هايدرازين كاربوثيوامايد

الخلاصة

تم تحضير المخلب الجديد 2-(2-ايمينو-1-مثيل ايميدازولدين-4-يل ادين) هايدرازين كاربوثيوامايد من تفاعل الكريـاتنيين مـع الثايوسـيميكاربزايد. تـم اختبـار كلوريدات لبعض العناصر الانتقالية الكروم الثلاثـي و [الكوبالـت، النيكـل, و النحـاس الثنائية] كاملاح نقية لتفاعلها وتعقيدها مع المخلب الجديد. تم التشخيص باستخدام الـرنين النووي المغناطيسي واطياف الأشـعة تحـت الحمـراء المعـززة بتحـويلات فـورير ، والأطياف الإلكترونية بالإضافة الى تحديد النسبة المولية ليكاند : فلز, فضلا عـن قيـاس العزم المغناطيسي المؤثر للمعقدات الصلبة, كما تم حسـاب اطـوال الاواصـر وزوايـا التاصروشحنة الذرة وحرارة التكوين باستخدام برنامج الكم اوفيس للمخلب الجديد كم وتم حساب استقرارية المعقدات الجديدة عن طريق نظرية دالة الكثافة. تـم دراسـة الفعاليـة المضادة للجراثيم لكل من الليكاندات ومعقداتها على خمسة أنـواع مـن البكتريـا هـي (Staphylococcus aureus, E. coli, Proteus Vulgaris, Pseudomonas, and Klebsiella pneumoniae).

* Applied Science Department, University of Technology / Baghdad

Introduction

The chemistry of thiosemicarbazones has received considerable attention in view of their variable bonding modes, promising biological implications, structural diversity, and ion-sensing ability [1–3]. They have been used as drugs and are reported to possess a wide variety of biological activities against bacteria, fungi, and certain type of tumors and they are also a useful model for bioinorganic processes [4–6]. The activity of these compounds is strongly dependent upon the nature of the heteroatomic ring and the position of attachment to the ring as well as the form of thiosemicarbazone moiety [7]. These are studied extensively due to their flexibility, their selectivity and sensitivity towards the central metal atom, structural and similarities with natural biological substances, due to the presence of imine group (−N=CH−) which imparts the biological activity [8-16]. This paper presents the synthesis and characterization of Cr(III), Co(II), Ni(II) and Cu(II) complexes with Schiff‹s base obtained by the reaction of 2-imino-1-methylimidazolidin-4-one with thiosemicarbazide.

Experiment

All chemical used were of reagent grade (supplied by either Merck or Fluka) and used as supplied. The FTIR spectra were recorded as CsI disc on FTIR 8300 Shimadzu Spectrophotometer. The UV-Visible spectra were measured using Shimadzu UV-Vis. 160 A spectrophotometer. Proton NMR spectra were recorded on Bruker - DPX 300 MHz spectrometer with TMS as internal standard in Jordan University. Magnetic susceptibility was measured by BM6 using Gouy's balance. Flame atomic absorption of elemental analyzer, shimadzu AA-670 was used for metal determination. Elemental micro analysis, was carried out using C.H.N elemental analyzer model 5500-Carlo Erba instrument.

Synthesis of ligand

This mixture of hot ethanolic solution of thiosemicarbazide (1.82 g, 0.02 mol) and creatinine (2-imino-1-methylimidazolidin-4-one) (2.26 g, 0.02 mol) were refluxed with stirring for 3 hours. The completion of the reaction was confirmed by the TLC. The reaction mass was degassed on a rotatory evaporator, over a water bath. Thiosemicarbazone (L) filtered, washed with cold EtOH, and dried under vacuum over P_4O_{10}. Proton NMR **(**1.8(1H) for NH, S. 2.2(3H) for CH_3, S. 2.7(2H) for CH_2, 8 for NH, 9.1 for NH, 10.9 for NH_2**).** Element chemical analysis data are shown in Table (1) [17], and the reaction equation was shown in scheme 1.

Synthesis of metal complexes

Bis(2-(2-imino-1-methylimidazolidin-4-ylidene)hydrazinecarbothioamide) metal complexes were obtained by refluxing the mixture of hydrated metal chlorides of Cr(III), Co(II), Ni(II), and Cu(II) (1 mmol) and 2 mmol of the ligand in 50ml ethanol at pH (8-9), till the complexes precipitated out. The colored complexes were filtered, washed with water, ethanol and dried under vacuum.

Study of complexes formation in solution

Complexes of ligand (L) with metal ions were studied in solution using ethanol (or DMF) as solvents, in order to determine (M:L) ratio in

the complex following molar ratio method [18]. A series of solution were prepared having a constant concentration 10^{-3} M of metal ion and different concentration of ligand (L). The [M/L] ratio was determined from relationship between absorption of the absorbed light and mole ratio of [M/L]. The results of complexes formation in ethanol (or DMF) were listed in table (2).

Study the biological activity for ligand (L) and its complexes

The biological activity of the prepared new ligand and its metal complexes were studied against selected types of bacteria which included positive bacteria (*Staphylococcus aureus*), and gram negative bacteria (*Escherichia coli*, *Klebsiella pneumoniae*, *Proteus vulgaris*, *Pseudomonas aeruginosa*), in brain hart broth agar media, which is used DMF as a solvent and as a control for the disc sensitivity test[19-21]. This method involves the exposure of the zone of inhibition toward the diffusion of micro-organism on agar plate. The plates were incubated for (24hr), at 37Cº. The antimicrobial activity was recorded as any area of microbial growth inhibition that occurred in the diffusion area.

Results and Discussion

The complexes were synthesized by reacting ligand with the metal ions in 1:2 molar ratio in ethanolic medium. The ligand behaves as bidentate coordinate through sulphur and nitrogen donor atoms (Figure 1).

I: UV/visible spectra: The U.V.-Visible of the ligand (L) and its metal complexes recorded in table(3). The solution of the ligand (L) in DMF exhibited two peaks at 255 and 322 nm (39215, 31055cm^{-1}) which are attributed to л л* or n л* . The red shift in solution of complexes were investigated depending upon л→ л* or→ n л* for all the complexes.

Cr-complex (C_1): The Uv-visible spectrum of the Cr(III) complex recorded in DMF showed three bands with the absorbance maxima at 43478 cm^{-1}, 26595 cm^{-1} and 16339 cm^{-1} which were considered as υ_1, υ_2, and υ_3 absorption bands respectively.

$\nu_1 = {}^4A_2g(F) \rightarrow {}^4T_1g(P)$
$\nu_2 = {}^4A_2g(F) \rightarrow {}^4T_1g(F)$
$\nu_3 = {}^4A_2g(F) \rightarrow {}^4T_2g(F)$

Co-complex (C_2): The electronic spectra of Co (II) complex showed two spin allowed transitions at 15527, and 28985 cm^{-1} assignable to $T_1g(F) \rightarrow A_2g(F)$ and $T^4{}_1g(F) \rightarrow T^4{}_2g(P)$ transitions respectively are in a good agreement with octahedral arrangements for Co(II) ion.

Ni-complex (C_3): The appearance of a band at 19047 cm^{-1} favors the tetrahedral geometry for the Ni (II) complex.

Cu-complex (C_4): Only one broad band is observed at 17699 cm^{-1} in the electronic spectrum of the Cu(II) complex assigned to $Eg^2 \rightarrow T_2g^2$ [22] transition which is in conformity with octahedral geometry.

II: FT.IR Spectroscopy

The FT.IR spectra provide valuable information regarding the nature of functional group attached to the metal atom. The ligand and metal complexes were characterized mainly

using the azomethine and primary amine ($-NH_2$) bands. The main infrared bands and their assignments are listed in Table 4. The appearance of a broad strong band in the IR spectra of the ligand in 3421cm^{-1} is assigned to N-H stretching vibrations of the primary amine group. The spectrum of the ligand shows two different –C=N bands at 1631 and 1618 cm^{-1}, which is shifted to lower frequencies in the spectra of all the complexes (1614-1575 cm^{-1}) indicating the involvement of –C=N nitrogen in coordination to the metal ion. The bonds attributed to (M-N) and (M-O) were observed in the region (468-521) and (395-440) cm^{-1} respectively in all complexes.

Stereochemistry of metal complexes

The two ligands are coordination sphere around the metal is significantly distorted from ideal octahedral geometry. To determine the coordination mode of the thiosemicarbazone ligands in these complexes, The structure shows that the thiosemicarbazone ligand is again coordinated to the metal in the same fashion as before. Formation of four- membered chelate ring, to determine the origin of such a four-membered ring formation, the stereochemistry of thiosemicarbazone was first taken into consideration. Owing to the restricted rotation around the C=N bond, the ligands may exist in two different geometric isomeric forms. The structure determination of one representative ligand, shows (Scheme 2) that the free ligand exists in thione form and corresponds to structure where the creatinine group is trans to the hydrazinic nitrogen across the C=N bond. Starting from the free ligand, five-membered chelate ring formation can take place, in principle, via rotation about the C–N (hydrazinic) single bond, followed by tautomerization to the thiol form and dissociation of the thiolate proton upon complexation complexes.

Stereo suggested structures of complexes

According to the above mentioned data (spectra, molar ratio and magnetic properties), the proposed structures of completes were shown in figures 1, 2:

Computer calculations

The data obtained for the minimized geometry, atomic charge, bond length, bond angle, dihedral angle, and heat of formation of the ligand were calculated using simiempirical AMI module in the CS chemoffice molecular modeling package.

These data show that the atomic charge (for the ligand) have been affected by the presence of substituent of rings as shown in data (Table 3-8). In figure 3, the data for minimized geometry (Table 3-8) and the 3d-geometrical structure is shown in. The data obtained show that the heat of formation is about 99.6Kcal, and the highest atomic charge in ligand molecule is at [(N-6) (-0.724)] the next charge value is at [(S-12) (-0.617)] and [(N-9)(-0.291)]. These data show clearly that these three atoms are the most reactive toward the bonding with the metal. The determined bond angle, dihedral angle and 3D-geometrical structure, indicate that this molecule is planar.

Stability study

The stability for the prepared complexes was studied theoretically by the Density Function Theory (DFT). The total energy for the complexes was calculated and it was shown that the copper complex is the most stable and the chromium complex is the least stable as follows: Cu-complex > Ni-complex > Co-complex > Cr-complex.

Biological activity

The antimicrobial screening data show that the compounds exhibit antimicrobial properties, and it is important to note that the metal chelates exhibit more inhibitory effects than the parent ligands. The increased activity of the metal chelates can be explained on the basis of chelation theory [22]. It is known that chelation tends to make the ligand act as more powerful and potent bactericidal agents, thus killing more of the bacteria than the ligand. It is observed that, in a complex, the positive charge of the metal is partially shared with the donor atoms present in the ligands, and there may be π-electron delocalization over the whole chelating [22]. This increases the lipophilic character of the metal chelate and favours its permeation through the lipoid layer of the bacterial membranes. The increased lipophilic character of these complexes seems to be responsible for their enhanced potent antibacterial activity. It may be suggested that these complexes deactivate various cellular enzymes, which play a vital role in various metabolic pathways of these microorganisms. It has also been proposed that the ultimate action of the toxicant is the denaturation of one or more proteins of the cell, which as a result, impairs normal cellular processes. There are other factors which also increase the activity, which are solubility, conductivity, and bond length between the metal and the ligand.

As a result from the study of antimicrobial of prepared ligand and it metal complexes, the following point were concluded:

1. The results of antibacterial activity study for 2-(2-imino-1-methylimidazolidin-4-ylidene)hydrazinecarbo thioamide dicated that the new ligand exhibited antibacterial activity against the studied bacteria at low and high concentration.

2. Generally, the result of prepared complexes exhibited antibacterial activity toward E. coli was more than the complexes inhibition on the other bacteria.

References

[1]-Casas JS, García-Tasende MS, Sordo J. *Coordination Chemistry Reviews.* 2000;**209**(1):197–261.

[2]-Mishra D, Naskar S, Drew MGB, Chattopadhyay SK. *Inorganica Chimica Acta.* 2006;**359**(2):585–592.

[3]-Kizilcikli I, Ülküseven B, Daşdemir Y, Akkurt B. *Synthesis and Reactivity in Inorganic and Metal-Organic Chemistry.* 2004;**34**(4):653–665.

[4]-Singh NK, Singh SB, Shrivastav A, Singh SM. *Proceedings of the Indian*

Academy of Sciences: Chemical Sciences. 2001;**113**(4):257–273.

[5]-Offiong OE, Martelli S. *Transition Metal Chemistry*. 1997;**22**(3):263–269.

[6]-Labisbal E, Haslow KD, Sousa-Pedrares A, Valdés-Martínez J, Hernández-Ortega S, West DX.. *Polyhedron*. 2003;**22**(20):2831–2837.

[7]-Singh RV, Fahmi N, Biyala MK. *Journal of the Iranian Chemical Society*. 2005;**2**(1):40–47.

[8]-Chandra S, Sangeetika, Rathi A. *Journal of Saudi Chemical Society*. 2001;**5**(2):175–182.

[9]-Raman, N., Kulandaisamy, A.; Shunmugasundaram, A.; Jeyasubramanian, K. Synthesis, spectral, redox and antimicrobial activities of Schiff base complexes derived from 1-phenyl-2,3-dimethyl-4-aminopyrazol-5-one and acetoacetanilide. *Transit. Metal Chem.* **2001,** *26*, 131-135.

[10]-Raman, N.; Kulandaisamy, A.; Jeyasubramanian, K. Synthesis, spectral, redox and antimicrobial activity of Schiff base transition metal(II) complexes derived from 4-aminoantipyrine and benzil.*Synth. React. Inorg. Met-Org. Nano-Met. Chem.* **2002,** *32*, 1583-1610.

[11]-Singh, L.; Sharma, D.K.; Singh, U.; Kumar, A. Synthesis and spectral studies of Cu(II) coordination compounds of 4[N-(cinnamalidene)amino]antipyrine semicarbazone. *Asian J.Chem.* **2004**, *16*, 577-580.

[12]-Raman, N.; Thangaraja, C.; Johnsonraja, S. Synthesis, spectral characterization, redox and antimicrobial activity of Schiff base transition metal(II) complexes derived from 4-aminoantipyrine and 3-salicylideneacetylacetone. *Centr. Eur. J. Chem.* **2005**, *3*, 537-555.

[13]-Pandey, O.P.; Sengupta, S.K.; Dwivedi, A. Organophosphorus derivatives containing antipyrine ring as chemotherapeutics against fungal pathogens of sugarcane. *Electron. J. Environ. Agr.Food Chem.* **2005**, *4*, 886-891.

[14]-Agarwal, R.K.; Singh, L.; Sharma, D. K. Synthesis, spectral and biological properties of copper (II) complexes of thiosemicarbazones of Schiff bases derived from 4-aminoantipyrine and aromatic aldehydes. *Bioinorg. Chem. Appl.* **2006**, article ID 59509.

[15]-Agarwal, R.K.; Gargb, R.K.; Sindhub, S.K. Synthesis and magneto-spectral investigations of some six and nine coordinated complexes of lanthanides(III) derived from 4[N-(2'-hydroxy-1'-napthalidene)amino]antipyrine thiosemicarbazone. *J. Iran. Chem. Soc.* **2005**, *2*, 203-211.

[16]-Agarwal R. K.; Prasad S. Synthesis and spectral investigations of some platinum metals ions coordination compounds of 4[N-(furan-2'-carboxalidene)amino]antipyrine thiosemicarbazoneand 4[N-(3',4',5'-trimethoxybenzalidene) amino]antipyrine thiosemicarbazone. *Turk. J. Chem*. **2005**, *29*, 289-29.

[17]-Sulekh Chandra, Smriti Raizada, Monika Tyagi, and

Archana Gautam, Bioinorg Chem Appl. 2007; 2007: 51483.
[18]- Rosu, T.; Pasculescu, S.; Lazar,
V.; Chifiriuc, C.; Cernat, R. Molecules 2006, 11, 904-914.
[19]-. Bothino F., Russo C., Blading
G., Farmaco Ed., Science, 298,37,1982.
[20]- SinghRV,Biyala MK, Fahmi N.
Important properties of sulfur-bonded organoboron (III) complexes with biologically potent ligands. Phosphorus, Sulfur and Silicon and the Related Elements. 2005;180(2): 425–434.
[21]-Costa RFF, Rebolledo AP, Matencio T, et al. Journal of Coordination Chemistry. 2005;58(15): 1307–1319.
[22]-Sengupta, S. K., Pandey, O. P., Srivastava, B. K. and Sharma, V. K., Transition Metal Chemistry, 1998,**23(4)**,pp.349–353

Table (1) Element chemical analysis data of the ligand

No.	Yield %	M.P. °C	Color	Chemical Formula	Elemental analysis calculated			Elemental analysis found		
					C%	H%	N%	C%	H%	N%
L	**70**	**153**	**Light brown**	**$C_5H_{10}N_6S$**	**32.25**	**5.41**	**45.12**	**31.91**	**5.11**	**44.74**

Table (2) Analytical data for the metal complexes

No.	Compound	Color	MP (°C)	Yield (%)	Elemental analysis calculated				Elemental analysis found			
					C%	H%	N%	M%	C%	H%	N%	M%
C_1	$CrL_2(H_2O)_2]Cl$	green	267	55	26.08	5.25	36.50	11.29	25.19	4.87	35.21	10.08
C_2	$[CoL_2(H_2O)_2]$	green	135	40	25.69	5.18	35.96	12.61	25.10	4.70	35.09	11.80
C3	$[NiL_2]$	brown	243	65	27.86	4.68	38.98	13.61	26.98	4.13	38.00	13.03
C4	$[Cu(H_2O)_2L_2]$	green	210	70	25.44	5.12	35.61	13.46	24.76	4.85	35.01	12.40

Table (3) Electronic spectra for ligand and complexes in ethanol solvent

No.	Compound	λmaxcm-1 (€max)	Magnetic moment μ (B.M)	Suggested Structure
L	$C_5H_{10}N_6S$	39215, 31055	-	-
C_1	$CrL_2(H_2O)_2]Cl$	43478, 26595, 16339	4.15	Octahedral
C_2	$[CoL_2(H_2O)_2]$	41666, 28985, 15527	4.25	Octahedral
C3	$Ni(L_2)_2.\ Cl_2$	45045, 25974, 19047	2.46	Tetrahedral
C_4	$[Cu(H_2O)_2L_2]$	40816, 28169, 17699	1.97	Octahedral

Table (4) Characteristic FT.IR bands (cm-1) of the compounds studied.

No.	NH_2	C=N	M-N	M-O
L	3421	1631	-	-
C_1	3409	1615	473	397
C_2	3412	1614	500	395
C_3	3385	1630	468	408
C_4	3398	1624	521	440

Table (5) The bond length of the ligand

Bond Length	Actual	Optima	Bond Length	Actual	Optima
N(1)-C(2)	1.4620	1.4620	N(9)-C(5)	1.2600	1.2600
N(1)-C(5)	1.4620	1.4620	N(6)-H(7)	1.0220	1.0220
N(1)-H(16	1.0500	1.0500	C(8)-H(18)	1.1130	1.1130
C(2)-N(3)	1.4620	1.4620	C(8)-H(19)	1.1130	1.1130
C(2)-N(6)	1.2600	1.2600	C(8)-H(20)	1.1130	1.1130
C(4)-N(3)	1.4700	1.4700	N(9)-N(10)	1.3520	-
C(8)-N(3)	1.4700	1.4700	N(10)-C(11)	1.3690	1.3690
C(4)-C(5)	1.6510	1.6510	H(17)-N(10)	1.0120	1.0120
C(4)-H(21)	1.1129	1.1129	S(12)-C(11)	1.5760	1.5760
C(4)-H(22)	1.1130	1.1130	N(13)-C(11)	1.3690	1.3690

Table (6) The bond angle of the ligand

Bond Angle	Actual	Optima	Bond Angle	Actual	Optima
H(14)-N(13)-H(15)	120.9334	118.8000	**C(4)-C(5)-N(9)**	121.0561	115.1000
H(14)-N(13)-C(11)	119.5344		**C(4)-C(5)-N(1)**	103.0780	125.3000
H(15)-N(13)-C(11)	119.5297		**H(22)-C(4)-H(21)**	115.7207	109.4000
S(12)-C(11)-N(10)	121.4300	121.4300	**C(5)-C(4)-H(21)**	109.4105	109.4100
N(13)-C(11)-N(10)	117.1343	120.0000	**N(3)-C(4)-H(21)**	107.5008	
S(12)-C(11)-N(13)	121.4329		**C(5)-C(4)-H(22)**	109.4078	109.4100
N(9)-N(10)-C(11)	120.8668		**N(3)-C(4)-H(22)**	107.4999	
H(17)-N(10)-N(9)	118.2650	117.4000	**N(3)-C(4)-C(5)**	106.9218	
C(5)-N(9)-N(10)	120.0002		**C(4)-N(3)-C(8)**	131.9981	
N(3)-C(8)-H(18)	107.5008		**C(8)-N(3)-C(2)**	119.9982	108.0000
N(3)-C(8)-H(19)	107.5006		**C(4)-N(3)-C(2)**	107.9998	108.0000
H(20)-C(8)-N(3)	107.4989		**N(3)-C(2)-N(6)**	122.9988	126.0000
H(18)-C(8)-H(19)	109.0004	109.0000	**N(1)-C(2)-N(6)**	125.9981	126.0000
H(20)-C(8)-H(18)	109.0003	109.0000	**N(3)-C(2)-N(1)**	110.9996	
H(20)-C(8)-H(19	116.0166	109.0000	**C(5)-N(1)-H(16)**	124.4978	118.0000
C(2)-N(6)-H(7)	110.0000	110.0000	**C(2)-N(1)-H(16)**	124.4981	118.0000
N(9)-C(5)-N(1)	135.8615	126.0000	**C(5)-N(1)-C(2)**	111.0006	124.0000

Table (7) The dihedra angle of the ligand

Dihedral Angle	Actual	Optima	Dihedral Angle	Actual	Optima
H(16)-N(1)	1.0500	1.0500	H(19)-C(8)-N(3)-C(2)	62.7837	
C(2)-N(3)	1.4620	1.4620	H(18)-C(8)-N(3)-C(2)	-179.9991	
N(6)-C(2)	1.2600	1.2600	H(20)-C(8)-N(3)-C(4)	118.0229	
C(4)-N(3)	1.4700	1.4700	H(19)-C(8)-N(3)-C(4)	-116.4106	
C(8)-N(3)	1.4700	1.4700	H(18)-C(8)-N(3)-C(4)	0.8066	
C(4)-C(5)	1.6510	1.4970	H(7)-N(6)-C(2)-N(1)	-0.0024	
H(21)-C(4)	1.1129	1.1130	H(7)-N(6)-C(2)-N(3)	-179.2660	
H(22)-C(4)	1.1130	1.1130	C(2)-N(1)-C(5)-C(4)	0.0578	
N(9)-C(5)	1.2600	1.2600	C(2)-N(1)-C(5)-N(9)	-179.1472	
H(7)-N(6)	1.0220	1.0220	H(16)-N(1)-C(5)-C(4)	179.4068	
H(18)-C(8)	1.1130	1.1130	H(16)-N(1)-C(5)-N(9)	0.2019	
C(8)-H(19)	1.1130	1.1130	N(3)-C(4)-C(5)-N(1)	-0.0937	
C(8)-H(20)	1.1130	1.1130	N(3)-C(4)-C(5)-N(9)	179.2600	
N(9)-N(10)	1.3520		H(22)-C(4)-C(5)-N(1)	-116.2253	
C(11)-N(10)	1.3690	1.3690	H(22)-C(4)-C(5)-N(9)	63.1284	
N(10)-H(17)	1.0120	1.0120	H(21)-C(4)-C(5)-N(1)	116.0405	
C(11)-S(12)	1.5760	1.5760	H(21)-C(4)-C(5)-N(9)	-64.6059	
C(11)-N(13)	1.3690	1.3690	C(5)-C(4)-N(3)-C(2)	0.0944	
N(13)-H(14)	1.0120	1.0120	H(22)-C(4)-N(3)-C(2)	117.4886	
H(15)-N(13)	1.0120	1.0120	H(21)-C(4)-N(3)-C(2)	-117.3033	
S(12)-C(11)-N(13)-H(15)	179.9768		C(5)-C(4)-N(3)-C(8)	179.3607	
S(12)-C(11)-N(13)-H(14)	-0.5993		H(22)-C(4)-N(3)-C(8)	-63.2451	
N(10)-C(11)-N(13)-H(15	0.5745		H(21)-C(4)-N(3)-C(8)	61.9630	
N(10)-C(11)-N(13)-H(14)	179.9984		N(1)-C(2)-N(3)-C(4)	-0.0621	
N(13)-C(11)-N(10)-H(17)	-120.5568		N(1)-C(2)-N(3)-C(8)	-179.4325	
S(12)-C(11)-N(10)-H(17)	60.0409		N(6)-C(2)-N(3)-C(4)	179.2997	
N(13)-C(11)-N(10)-N(9)	59.9984		N(6)-C(2)-N(3)-C(8)	-0.0707	
S(12)-C(11)-N(10)-N(9)	-119.4039		C(5)-N(1)-C(2)-N(3)	-0.0026	
C(5)-N(9)-N(10)-H(17)	60.5691		C(5)-N(1)-C(2)-N(6)	-179.3411	
C(5)-N(9)-N(10)-C(11)	-120.0005		H(16)-N(1)-C(2)-N(3)	-179.3517	
N(10)-N(9)-C(5)-C(4)	-179.0908		H(16)-N(1)-C(2)-N(6)	1.3098	
N(10)-N(9)-C(5)-N(1)	0.0051		H(20)-C(8)-N(3)-C(2)	-62.7828	

Table (8) Atomic charge of the ligand.

Charges	Charges	Charges	Charges	Charges	Charges
N 0.035 [N(1)]	C 0.187 [C(5)]	N 0.071 [N(10)]	H 0.093 [H(16)]	H 0.042 [H(18)]	H 0.099 [H(14)]
C 0.370 [C(2)]	N -0.724 [N(6)]	C 0.303 [C(11)]	H 0.030 [H(21)]	H 0.031 [H(19)]	H 0.099 [H(15)]
N 0.083 [N(3)]	C -0.059 [C(8)]	S -0.617 [S(12)]	H 0.029 [H(22)]	H 0.031 [H(20)]	
C -0.049 [C(4)]	N -0.291 [N(9)]	N 0.017 [N(13)]	H 0.123 [H(7)]	H 0.097 [H(17)]	

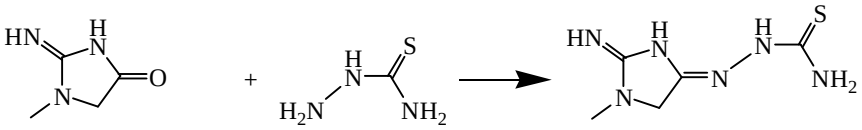

Creatinine **(L)**

Scheme 1: Formation of the ligand

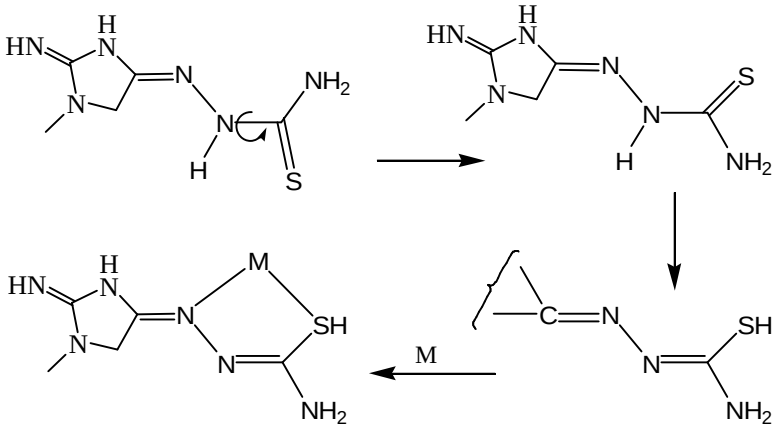

Scheme 2: Probable steps involved in the formation of five-membered chelate rings

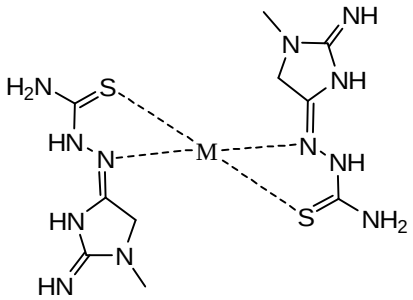

Figure 1: Structures of the complexes.

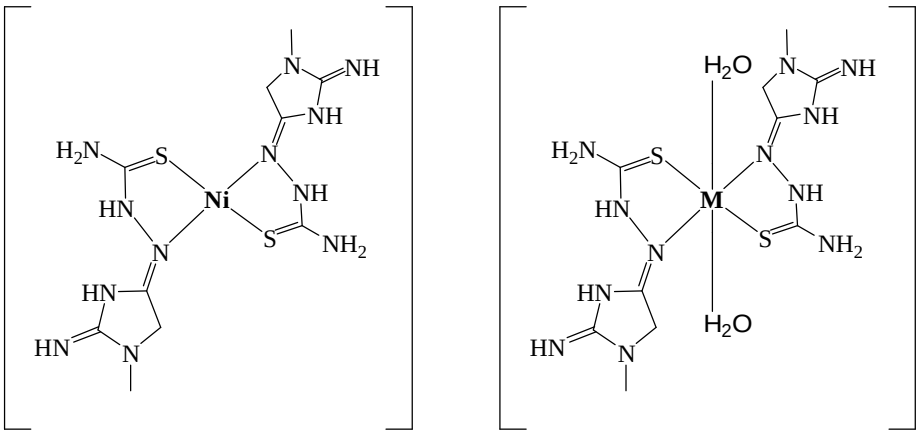

Structure (I): Square planer geometry of Ni(II) complex.

Structure (II): Octahedral geometry of C_1, C_2, C_4 complexs.

Figure 2: The structurs of our complexes.

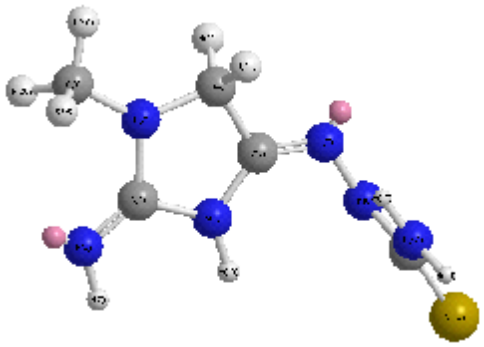

Stereochemistry: C(5)-N(9): (Z)
Bend: 11.9559
Dipole/Dipole: -5.7927
Torsion: 1.7144
Stretch-Bend: -0.1293

Figure 3: The three dimentiona structure of the ligand

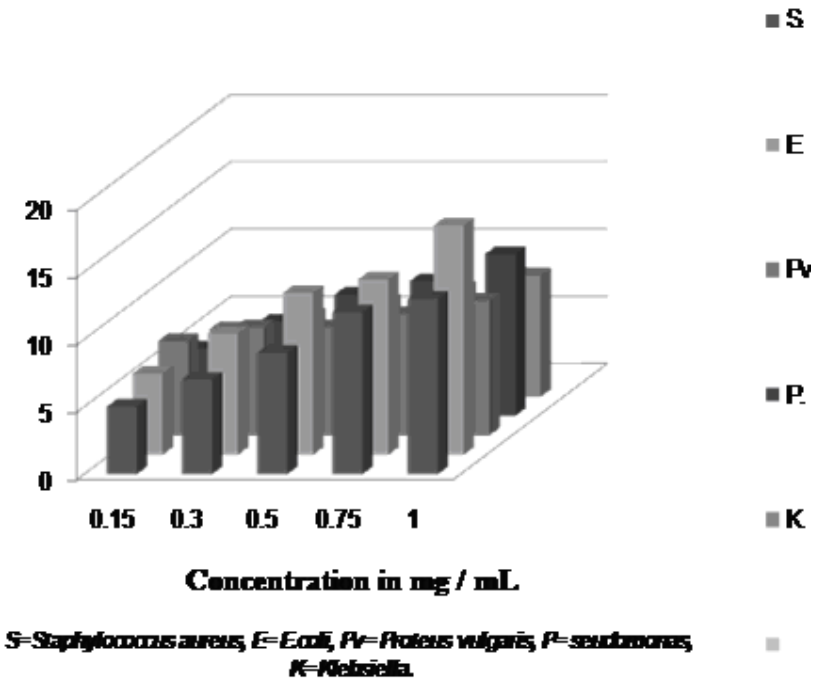

Figure 4: The Effect of Test Organism Toward Ligand

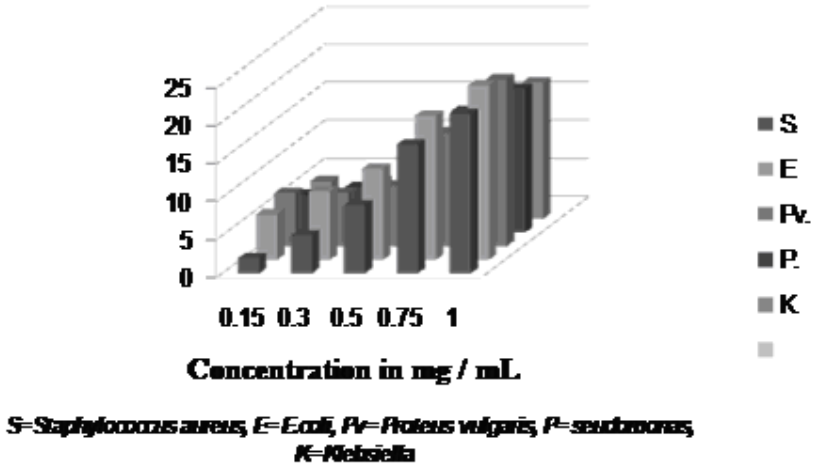

Figure 5: The Effect of Test Organism Toward C1-Complex

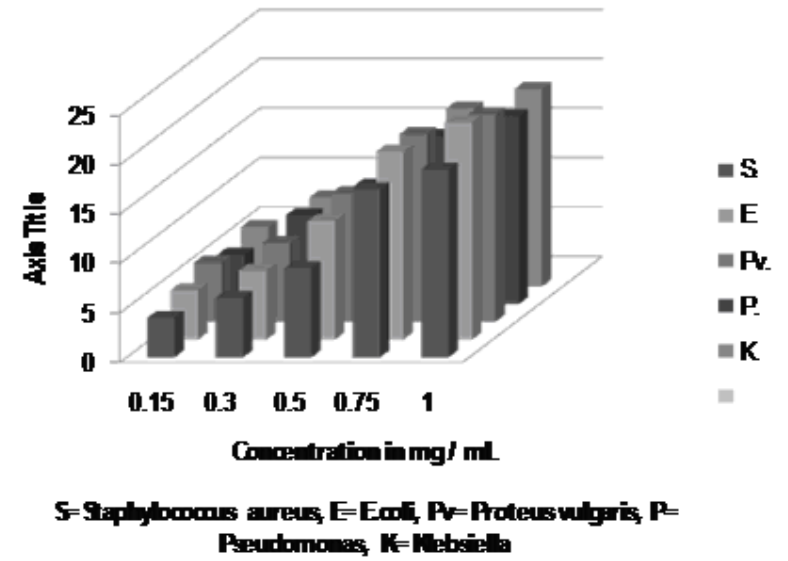

Figure 6: The Effect of Test Organism Toward C2-Complex

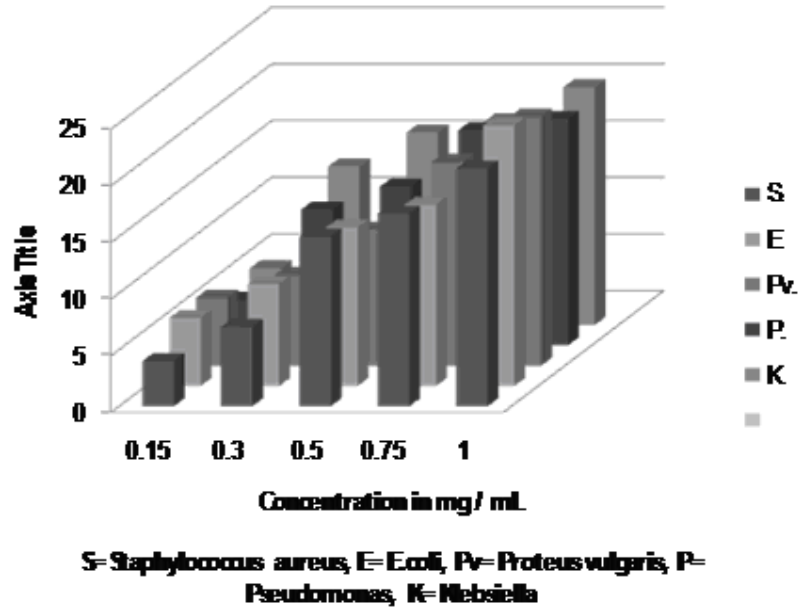

Figure 7: The Effect of Test Organism Toward C3-Complex

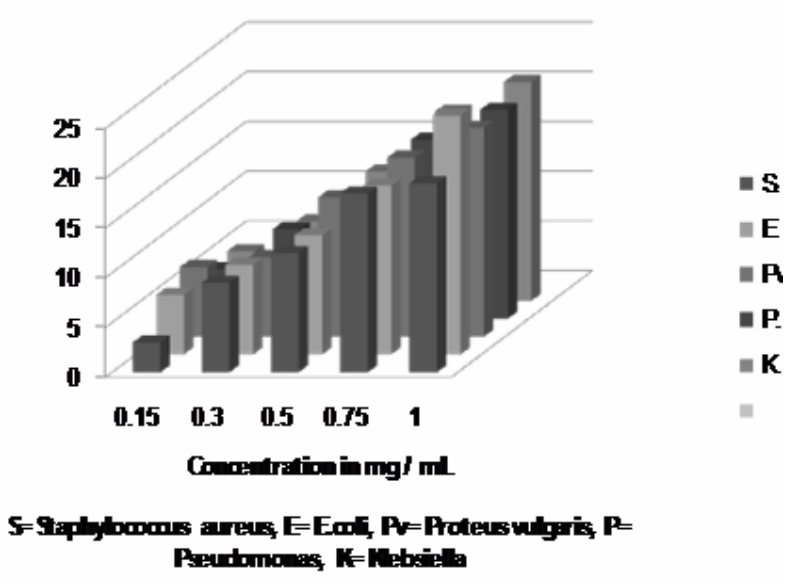

Figure 8: The Effect of Test Organism Toward C4-Complex